International Journal of Control, Automation and Systems 20(5) (2022) 1745-1755
http://dx.doi.org/10.1007/s12555-020-0115-4
ISSN:1598-6446 eISSN:2005-4092
http://www.springer.com/12555

SD-TCSs Control Deriving from Fractional-order Sliding Mode and Fuzzy-compensator

Sy Dzung Nguyen* **and Vien Quoc Nguyen**

Abstract: Uncertainty and disturbance (UAD) always exist and influence negatively on technical systems. Focusing on improving the effectiveness of smart dampers (SDs)-based semi-active train-car suspensions (SD-TCSs), we present the fuzzy-compensator-enhanced fractional-derivative (FD) order sliding control of a class of SD-TCSs subjected to UAD, in which the disturbance time-varying rate (DTVR) may be high but bounded. To reduce uncertainty related to the mathematical model error, we propose a fractional derivative (FD)-based sliding mode controller (FDSMC) for specifying the main control signal. Whereas, to estimate the compensation for external disturbance, first, we utilize the well-known DO to build an initial framework of the compensator. To avoid conflict between the update-laws of the DO and FDSMC, as well as to make the system dynamic response converge stably to the desired state even if the DTVR increasing but bounded, constraints along with a fuzzy-based adjusting mechanism are then discovered. Thus, we obtain an improved DO (imDO), update-laws of the imDO and FDSMC, and their combination model (imDO-FDSMC) of the proposed controller. The survey results reflect the positive capability of the method.

Keywords: Disturbance observer (DO), fractional-order sliding control, magneto-rheological damper (MRD), MRD train-car suspensions.

1. INTRODUCTION

Smart dampers (SDs), for example, the magneto-rheological damper (MRDs) has been widely applied to vibration control systems [1]. To control SD-based suspensions well, together with the building reasonable control strategies, seeking appropriate solutions for preventing the negative impact of UAD is also vital. The lack of accuracy of the measurement devices and methods, the error of mathematical models describing the systems, including the hysteretic dynamic response of the smart fluids, and the unknown influence of the surrounding environment on the systems are the main causes of UAD [2–5]. In this study we concern with the control of SD-TCSs subjected to UAD whose DTVR may be high but bounded. Better depicting the system's dynamic response to reduce the model error, and quantifying compensation for UAD closer to its real influence are considered.

Obviously, the negative participation of unknown aspects or uncertainty features results in inaccuracy in the generated control signal. Therefore, many disturbance observers (DO) have been discovered to deal with this issue [4,5]. The well-known DO [5] has been applied effectively to several fields such as controlling ballistic trajectory or vibration. One can refer to the control of a class of smart suspensions subjected to UAD in [4]. It consisted of a sliding mode controller (SMC) and a lumped disturbance observer. However, the controllers [4,5] could be seen as tools fit for only the cases of the DTVR very low. Recently, applications of fractional calculus have been rapidly growing in the fields of physics, applied mathematics, engineering, and also in nonlinear control [6–13]. Being different from the traditional ways, fractional calculus deals with arbitrary order derivatives and integrations [6–9]. With the participating of FD, the complex nature of many technical systems can be more precisely modeled [6–8]. This can be seen as an approach to mitigate UAD. Although fractional operators provide significant advantages for the nonlinear control field, the stability analysis for the closed-loop systems is very difficult related to the derivative properties [10]. There have been some solutions to overcome this issue partly. The theoretical basis developments in [10,11] allowed to preserve the most interesting and useful FD properties, even in the case of not neces-

Manuscript received February 11, 2020; revised August 25, 2020, December 24, 2020, and April 29, 2021; accepted August 2, 2021. Recommended by Associate Editor Truong Quang Dinh under the direction of Editor Kyoung Kwan Ahn. This research is funded by Vietnam National Foundation for Science and Technology Development (NAFOSTED) under Grant Number 107.01-2019.328.

Sy Dzung Nguyen is with Division of Computational Mechatronics, Institute for Computational Science, Ton Duc Thang University, Ho Chi Minh City, Vietnam; Faculty of Electrical and Electronics Engineering, Ton Duc Thang University, Ho Chi Minh City, Vietnam (e-mail: nguyensydung@tdtu.edu.vn). Vien Quoc Nguyen is with Industrial University of Ho Chi Minh City, Vietnam (e-mail: nguyenvienquoc@iuh.edu.vn).
* Corresponding author.

sarily integer-order differentiable functions. Another way regarding the FD-based control systems with their derivative order very close to the integer-order can be referred to in [6,8]. In these, for simplicity, one combined the properties of the integer- and fractional-order systems in analyzing the asymptotic stability of quadratic Lyapunov functions to seek control laws. Besides, reality has shown that fuzzy logic is a flexible tool; it allows modification in the rules and even dealing with imprecise, distorted, and error input information. This, hence, has inspired researchers in seeking suitable solutions for challenges coming from the control of nonlinear systems in the presence of UAD [14–16]. Especially, a combination of fuzzy logic, FD, and SMC can be set up to exploit their advantages [6–8].

SMC takes the role of a framework to set up control laws. The main advantages of SMC are the robustness against uncertainty, the adaptive ability to deal with external disturbance, and the simplicity in implementation [1,17]. Theoretically, from a sliding surface expressing the control aim, the first phase (or the reaching one) starts from a certain initial condition and moves towards the sliding surface. It finishes as the trajectory converging to the sliding surface to begin the second phase (sliding phase). The fast response time in the first phase and the stability of holding or adhesion to the sliding surface in the second phase reflects the quality of SMC [1,2]. In the ideal case without UAD, the system states often move along the sliding surface. So, for simplicity, linear functions with constant parameters are the fit option to depict this surface [18]. In fact, due to always existing UAD, imperfections in the control action deriving from UAD often result in the chattering status [19]. To face this, rather than forcing the states to remain on the sliding surface like the ideal case, one only requires them to move in a certain neighborhood close enough to the sliding surface. Also, different kinds of sliding surfaces have been proposed, such as the constant nonlinear [20], nonlinear discrete moving [21], or nonlinear continuous moving one [22]. Generally, sliding surfaces can be classified into two groups: the linear sliding surfaces (LSSs) and the moving nonlinear sliding surfaces (MNSSs). Despite the simplicity, the use of the LSSs has certain disadvantages. For instance, the control signal required to keep the system states on or in the neighborhood of the LSSs usually increases in direct proportion to the magnitude of the tracking error. This may exceed the responding ability of actuators. Another problem often arises when states of the controlled system touch the surface. As usual, at this time and the next duration, the dynamic characteristics of the controlled system are often replaced by that of the sliding surface to estimate the control laws; so, for LSS, it is difficult to seek a replacement fit enough. In this context, MNSS can take the role better [23]. Also, MNSS-based algorithms can lessen the reaching time as well as improve the stability in the second phase. However, for such an MNSS, there exist difficulties in describing and determining its time-varying parameters. Moreover, setting up the control law and quantifying the stability boundaries are also challenges [17]. The problem here is how to exploit the advantages of both, LSS and MNSS, for the control of SD-TCSs.

So far, applications of FD for smart suspension systems have concentrated on either describing equipment participating in the systems such as [12,13] or establishing nonlinear control laws as in [6,8]. A combination of the strong points of the LSS and MNSS performed through the FD-based nonlinear sliding surfaces was shown in [6,8]. In these, by using optimal derivative-orders, the FD-based sliding surfaces in the form of an LSS were able to reflect the global dynamics of the controlled systems better than that of the traditional LSS and more simply than the MNSS. The different control laws for SD-TCSs, a half-car model, were discovered. Thus, they could control more effectively to minimize the translational and rotational chassis vibrations independently [6] or compromisingly [8]. However, the two methods had to rely on the assumption that there existed certain methods to estimate UAD accurately. So, the following problems make our research motivation.

1) How to develop an FD-based controller for SD-TCSs including a DO which can quantify the compensation converging to the wanted value to mitigate the negative impact of UAD?
2) What are the important observations/notes when using FD for the control field?

Consequently, in this paper, we present a fractional-order sliding controller enhanced by a compensator for a class of SD-TCSs, quarter-railroad-car model, subjected to UAD whose DTVR may be high but bounded. The controller named imDO-FDSMC is a combination of an improved DO (imDO), deriving from the DO presented in [4], and an FD-based SMC (FDSMC). First, an FD-based nonlinear sliding surface is defined, from which the control and update laws are then developed. In this process, FD takes part in reducing uncertainty status related to the mathematical model error. To build the compensator, first, we build its initial framework; two solutions for ensuring the effectiveness of the method are then proposed. The first one relates to a constraint mechanism to avoid conflict between the update laws of the DO and FDSMC. The second one is an adaptive fuzzy law (AFL) for enhancing the stable zero-convergence ability of the sliding surface.

The main contributions in this paper are as follows: The first one is the proposed initial framework of the controller described via the FD-based SMC (see Theorem 1). This makes advantages of the FDSMC compared with the traditional SMC as in [1,4,24] in mitigating model error. The second is the proposed constraint mechanism and the AFL to set up the update laws of the imDO and FDSMC (see Theorem 2). Thus, the imDO-FDSMC can overcome the

difficulty of the method [4] when facing with UAD whose DTVR may be high but bounded. Also, the imDO is seen as a supplement to the assumptions set out in [6,8]. The last one comes from the surveys and conclusion in Sections 4 and 5 which provide application-oriented information for the FD in the control field.

2. ISSUE FORMULATION AND APPROACH

2.1. Mathematical model of the survey object

We build a quarter-railroad-car model via a controllable bogie considering the impact of the rails, precast concrete panels, and concrete support layers on the system dynamic response. Fig. 1(a) depicts the bogie shown in http://passion-trains.over-blog.com/article-8965339.html.

The primary and secondary suspensions are the main systems for stamping out the vibration of the railroad car. In bogies of high-speed railroad cars, smart suspensions are often used. Let consider a smart bogie using an MRD installed in the secondary suspension. To build its mathematical model, we employ the dynamic analysis model

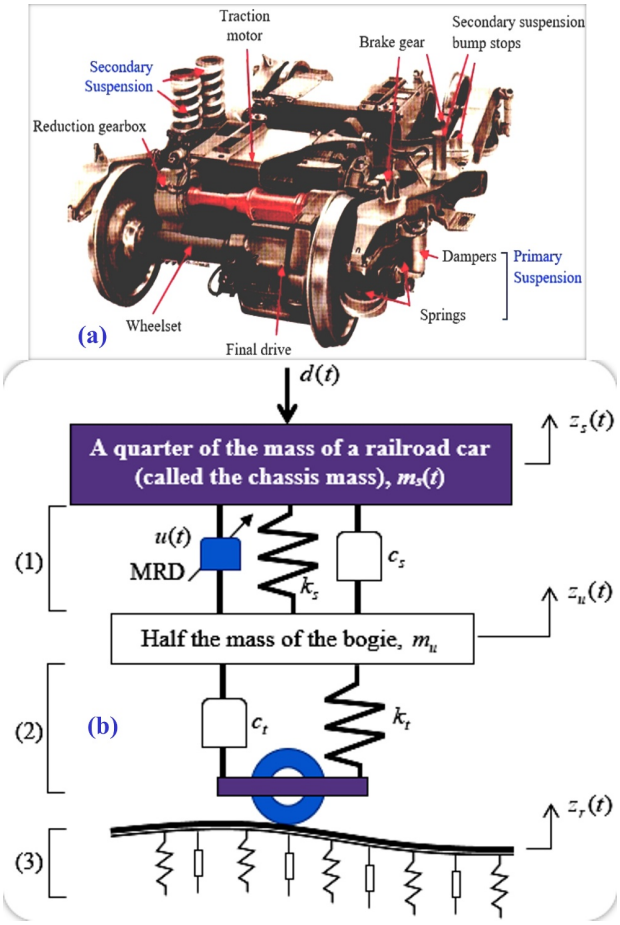

Fig. 1. (a) Structure of the bogie and (b) the proposed MRD-based suspension quarter-railroad-car model.

of a vehicle-track coupling system showed in [25]. Each rail, precast track slab, and the concrete support layer is modeled as a 2D-beam element with the corresponding continuous viscoelastic support. By using equivalent viscoelastic factors, we describe each half of the bogie as a quarter-railroad-car model as in Fig. 1(b), where (1) and (2), respectively correspond to the secondary and primary suspensions in Fig. 1(a); while (3) is the area to be constituted of the rails, precast concrete panels, and concrete support layers. In area (1), the equivalent spring stiffness and damping coefficients are denoted by k_s and c_s; the MRD is installed here to create control force $u(t)$. In areas (2) and (3), the viscoelastic behavior from the continuous viscoelastic support of the rails, track slabs, and concrete layer impacts directly on the the primary suspension. Therefore, we denote the stiffness and damping coefficients of area (2) considering the impact coming from area (3) by equivalent stiffness and damping coefficients k_t and c_t, respectively. Thus, uncertainty due to the model error always exists. We thereby denote all the unknown lumped model error and external disturbance by time parameter $d(t)$.

The volume acting on half of the bogie in Fig. 1(a) is the sprung mass or chassis mass $m_s(t)$ in Fig. 1(b). It is constituted of the passenger mass, cargo mass, the vertical aerodynamic component, and the mass of the framework. This is an unknown time-varying parameter. The known unsprung mass m_u includes the wheels, shaft, brakes, suspension linkage, and so on. The vertical displacement of m_s, m_u and the track profile are denoted by z_s, z_u and z_r. The spring and damper forces generated by k_s, k_t, c_s, c_t are f_s, f_{ts}, f_d, f_{td}. The controller has to estimate $u(t)$ to stamp out chassis vibration.

Assumption 1: There exists a known thresholds of $m_s(t) : \underline{m}_s = \min(m_s(t))$ and $\overline{m}_s = \max(m_s(t))$,

$$\underline{m}_s \leq m_s(t) \leq \overline{m}_s. \tag{1}$$

Assumption 2: Related to the spring stiffness and damping coefficients, k_s and c_s are observable; $k_t = k_t(t)$ and $c_t = c_t(t)$ are time-varying parameters unknown and bounded.

Assumption 3: For UAD, the uncertainty comes from the model errors while the disturbance relates to two sources. The first is the random change in the load including the vertical aerodynamic component which participates in $m_s(t)$. The second derives from the unstable support of the rails, track slabs, and concrete support layer which relates to the unknown $k_t = k_t(t)$ and $c_t = c_t(t)$. All the lumped UAD is denoted by $d(t)$ as in Fig. 1(b). The time-varying rate of $d(t)$ may be high but bounded by a known value, $|\dot{d}(t)| < \Omega$.

Be noted that to design technique systems, generally, one has to know at least the maximum and minimum thresholds of the related technical parameters; from these

thresholds, their normal values are estimated. Here, actually, the unknown $m_s(t)$, $k_t = k_t(t)$ and $c_t = c_t(t)$ impact directly on the suspension. However, their known nominal values m_{sn}, k_{tn} and c_{tn}, respectively, are used to calculate the main part in $u(t)$, the error is then estimated to compensate. These aspects reflect the reasonability of the above assumptions.

2.2. Issue formulation and solution

For a quarter car model, the suspension system can be depicted via a state vector $\mathbf{x}(t)$ as follows:

$$\begin{cases} \dot{\mathbf{x}}(t) = \mathbf{f}(\mathbf{x},t) + \mathbf{g_1}(t)u(t) + \mathbf{g_2}(t)d(t), \\ y(t) = x_1(t), \end{cases} \tag{2}$$

where $x(t) = \begin{bmatrix} x_1, & x_2, & x_3, & x_4 \end{bmatrix}^T = \begin{bmatrix} z_s, & \dot{z}_s, & z_u, & \dot{z}_u \end{bmatrix}^T$, and

$$\begin{cases} \mathbf{f}(\mathbf{x},t) = \begin{bmatrix} x_2(t) & -\frac{F_{sd}}{m_s(t)} & x_4(t) & \frac{F_{sd}-F_r}{m_u} \end{bmatrix}^T, \\ \mathbf{g_1}(t) = \begin{bmatrix} 0 & -\frac{1}{m_s(t)} & 0 & \frac{1}{m_u} \end{bmatrix}^T, \\ \mathbf{g_2}(t) = \begin{bmatrix} 0 & \frac{1}{m_s(t)} & 0 & 0 \end{bmatrix}^T, \end{cases} \tag{3}$$

$$F_{sd} = f_s + f_d = k_s(x_1 - x_3) + c_s(x_2 - x_4), \tag{4}$$

$$F_r = f_{ts} + f_{td} = k_{tn}(x_3 - z_r) + c_{tn}(x_4 - \dot{z}_r), \tag{5}$$

$$u(t) = u_s(t) + u_c(t). \tag{6}$$

In the above, $u_s(t)$ is used for controlling the system (2) without UAD, while $u_c(t)$ compensates for UAD.

There are two issues related to (6). In many cases, the solution (6) to the system (2) is sought via integer-order-derivative-based depictions. Reality has shown that due to the complexly natural attributes of technology systems, this approach lacks in accuracy [6,8,13], which results in increasing uncertainty or the model error. To overcome partly this issue, we exploit FD. The second issue relates to the compensation. The well-known disturbance observer DO [5] has been seen as a tool fit only for the time-varying rate of disturbance to be very low or $\dot{d}(t) \approx 0$ [4,5]. In this study, we focus on the case DTVR may be high but bounded. For this aim, we propose a solution for improving DO.

3. DESIGN OF THE PROPOSED CONTROLLER

Lemma 1 [7]**:** Let $X(t) \in \mathcal{R}$ be a continuous and derivable function. For any time instant $t \geq t_0$ and $\forall \alpha \in (0,1)$, then $0.5{}_{t_0}^{C}D_t^{\alpha} X^2(t) \leq X(t){}_{t_0}^{C}D_t^{\alpha} X(t)$.

Property 1 [9]**:** Let $C^1[a,b]$ denote the space of continuously differentiable functions on $[a, b]$. If $X(t) \in C^1[a,b]$ for some $b > a \geq 0$, then for $t \in [a, b]$,

$${}^{C}D_{a^+}^{\alpha_2}{}^{C}D_{a^+}^{\alpha_1} X(t) = {}^{C}D_{a^+}^{\alpha_1}{}^{C}D_{a^+}^{\alpha_2} X(t) = {}^{C}D_{a^+}^{\alpha_1+\alpha_2} X(t),$$

where $\alpha_1, \alpha_2 > 0$ and $\alpha_1 + \alpha_2 \leq 1$.

3.1. The initiation of the imDO-FDSMC

We define an FD-based sliding surface as below.

$$S(\mathbf{x},t) = k_1 x_1(t) + {}^{C}D_t^{1-\alpha} x_2(t), \tag{7}$$

where $\alpha \in (0, 1)$ and k_1 is a positive coefficient, the initiation of the imDO-FDSMC is depicted as follows.

Theorem 1: System (2) subjected to UAD is controlled by $u(t)$ (6) as detailed below

$$u_s(t) = k_1 m_s(t) {}^{C}D_t^{\alpha} x_1(t) - F_{sd} + k_2(t) m_s(t) \text{sat}(S(\mathbf{x},t)), \tag{8a}$$

$$u_c(t) = \hat{d}(t), \tag{8b}$$

where $\hat{d}(t)$ is the estimate of $d(t)$. If $\hat{d}(t) \to d(t)$, then $(x_1(t), x_2(t)) \to 0$ is a stable Lyapunov proccess.

Proof: From Property 1 and (7), it can be infer that for any $b > a \geq 0$ and $t \in [a, b]$, the fractional-order derivative of $S(\mathbf{x},t)$ with respect to time as in (9) always exists.

$$\begin{aligned} {}^{C}D_t^{\alpha} S(\mathbf{x},t) &= k_1 {}^{C}D_t^{\alpha} x_1(t) + \dot{x}_2(t) \\ &= k_1 {}^{C}D_t^{\alpha} x_1(t) - \frac{F_{sd}}{m_s(t)} - \frac{u_s(t)}{m_s(t)} + \frac{d(t)}{m_s(t)}. \end{aligned} \tag{9}$$

A Lyapunov candidate function is defined as

$$V_1(1) = 0.5 S^2(\mathbf{x},t). \tag{10}$$

From (10) and Lemma 1, we get

$${}^{C}D_t^{\alpha} V_1(t) = 0.5 {}^{C}D_t^{\alpha} S^2(\mathbf{x},t), \tag{11}$$

$${}^{C}D_t^{\alpha} V_1(t) \leq S(\mathbf{x},t) {}^{C}D_t^{\alpha} S(\mathbf{x},t). \tag{12}$$

Due to $V_1(t) \geq 0 \ \forall t$, we can infer from (12) that to $(x_1(t), x_2(t)) \to 0$ is a Lyapunov stable process, control law $u(t)$ in (2) must be updated such that

$${}^{C}D_t^{\alpha} = -k_2(t) \text{sgn} S(\mathbf{x},t), \ \forall k_2(t) > 0. \tag{13}$$

From (9) and (13), the following is yielded.

$$u(t) = k_1 m_s(t) {}^{C}D_t^{\alpha} x_1(t) - F_{sd} + k_2(t) m_s(t) \text{sgn} S(\mathbf{x},t) + d. \tag{14}$$

In case $\hat{d}(t) \to d(t)$ and sgn(.) is replaced by sat(.) as in (15) to prevent chattering, (14) then becomes (16) with the two parts as in (8).

$$\text{sat}(\Xi) = \begin{cases} \text{sgn}(\Xi), & \text{if } |\Xi| \geq 1, \\ \Xi, & \text{if } |\Xi| < 1. \end{cases} \tag{15}$$

Remark 1: To infer (13), we i) relied on the properties of integer-order derivative, and ii) had to assume that the integer-order differentiability condition of $S(\mathbf{x},t)$ was satisfied. This way has been exploited in [6,8]. Fortunately,

through the survey shown in Section 4, we found that with the system (2), the optimal value of alpha is 0.95 to be very close to 1, so the difference between the integer- and fractional-order properties is faded; besides, as shown in Fig. 5 (Section 4), the differentiability of $S(\mathbf{x},t)$ is almost fulfilled. This approach is fit for some systems, including the one (2). However, it should be better to analyze the stability of a more general class of fractional-order nonlinear systems upon the Mittag–Leffler stability such as the methods shown in [10,11].

3.2. The structure of the compensator

Based on the theory shown in [5], the initial structure of the DO for system (2) is depicted as in (16)-(19) [4].

$$\hat{d}(t) = z(\mathbf{x}(t),t) + \mathbf{l}(\mathbf{x}(t))\mathbf{x}(t), \tag{16}$$

$$\mathbf{l}(\mathbf{x}(t)) = [0,\ l_2(t),\ 0,\ 0], \tag{17}$$

$$\dot{z}(\mathbf{x},t) = -\frac{l_2(t)}{m_s(t)} z(\mathbf{x},t) - \mathbf{l}(\mathbf{x}(t))\mathbf{M}(\mathbf{x}(t),u(t)), \tag{18}$$

$$\mathbf{M}(\mathbf{x}(t),u(t)) = \begin{bmatrix} x_2 \\ m_s^{-1}(\mathbf{l}(\mathbf{x}(t))\mathbf{x}(t) - F_{sd} - u(t)) \\ x_4 \\ m_u^{-1}(F_{sd} - F_r + u(t)) \end{bmatrix}. \tag{19}$$

For this DO, the condition for $e(t) \to 0$ is $\dot{d}(t) \to 0$;

$$e(t) = d(t) - \hat{d}(t). \tag{20}$$

Remark 2: We focus on $\dot{d}(t) \neq 0$ but $|\dot{d}(t)| < \Omega$ contrasting to $\dot{d}(t) \to 0$ of the DO [4,5]. So, to exploit (16)-(19), Theorem 2 will supplement new constraints between the update-rules of $u_s(t)$ (8) of the FDSMC and $u_c(t) = \hat{d}(t)$ (16) of the DO to obtain the improving DO (imDO) in the combination form imDO-FDSMC.

3.3. The imDO-FDSMC

From $S(\mathbf{x},t)$ (7) and $DS(\mathbf{x},t)$ (9), we propose update-laws for $k_2(t)$ and $l_2(t)$ as in (21) and (22).

$$\begin{cases} k_2(t) = \bar{k}_2 \dfrac{S^2(\mathbf{x},t) + \Omega^2}{\xi + 2\underline{m}_s |S(\mathbf{x},t)|},\ \bar{k}_2 > 1, \\ l_2(t) = k_l \overline{m}_s,\ k_l > 1, \end{cases} \tag{21}$$

where $0 < \xi \ll 1$ is an arbitrarily chosen parameter.

$$\begin{aligned} &\text{AFL: IF } S \geq 0 \text{ AND } DS \geq 0, \text{ or} \\ &\quad \text{IF } S < 0 \text{ AND } DS < 0, \\ &\quad \text{THEN } k_2(t) = \text{UD via (21)}; \\ &\quad \text{Otherwise, } k_2(t) = \text{NC}. \end{aligned} \tag{22}$$

The adaptive fuzzy law (AFL) (22) illustrated in Fig. 2 is adopted for $k_2(t)$ only. NC denotes 'No Change' or to be maintained equal to the value in the previous loop; UD (Updated) means $k_2(t)$ to be updated as (21).

DS \ S	-	+
-	UD	NC
+	NC	UD

Fig. 2. The fuzzy relation for updating $k_2(t)$.

Theorem 2: System (2) subjected to UAD satisfying Assumption 3 is controlled by law (6), in which $u_s(t)$ is specified by (8), and $u_c(t) = \hat{d}(t)$ is specified by (16). If $l_2(t) = k_l \overline{m}_s$, $k_l > 1$, and $k_2(t)$ is updated by law (22) then the convergence to zero of the chassis' vertical vibration is a Lyapunov asymptotically stable process.

Proof: Be noted that in both the followings: i) $S(\mathbf{x},t) > 0$ but ${}^C D_t^\alpha S(\mathbf{x},t) < 0$, and ii) $S(\mathbf{x},t) < 0$ but ${}^C D_t^\alpha S(\mathbf{x},t) > 0$ corresponding to the areas 'NC' in Fig. 2, the varying tendency of the sliding surface to be $S(\mathbf{x},t) \to 0$. So, there is not any change in the control signal to be performed. Otherwise, related to 'UD' in Fig. 2, the control signal must be updated to force $S(\mathbf{x},t) \to 0$. This work is carried as below.

From (7), taking note of (2)-(5), we obtain

$${}^C D_t^\alpha S(\mathbf{x},t) = k_1 {}^C D_t^\alpha x_1(t) - \frac{1}{m_s(t)}[F_{sd} + u(t) - d(t)]. \tag{23}$$

From (6), (8), and (20), equation (23) becomes

$${}^C D_t^\alpha S(\mathbf{x},t) = k_2(t)\text{sat}S(\mathbf{x},t) + \frac{e(t)}{m_s(t)}. \tag{24}$$

By taking note of (16)-(20), we get

$$\dot{e}(t) = \dot{d}(t) - \mathbf{l}(\mathbf{x})\mathbf{g}_2 e(t). \tag{25}$$

A trade-off between the update-laws of the FDSMC and imDO is infered via Lyaponov function (26).

$$V_2 = 0.5S^2(x,t) + \frac{e^2(t)}{2\overline{m}_s} \geq 0, \tag{26}$$

$$\dot{V}_2 = S(\mathbf{x},t)\dot{S}(\mathbf{x},t) + \frac{e(t)\dot{e}(t)}{\overline{m}_s}. \tag{27}$$

Due to $\alpha \in [0.9,\ 1]$, from Lemma 1 it can infer that in both the areas signed UD in Fig. 2, $0 \leq S(\mathbf{x},t)\dot{S}(\mathbf{x},t) \leq S(\mathbf{x},t){}^C D_t^\alpha S(\mathbf{x},t)$. So

$$\dot{V}_2 \leq A = S(\mathbf{x},t){}^C D_t^\alpha S(\mathbf{x},t) + \frac{e(t)\dot{e}(t)}{\overline{m}_s}. \tag{28}$$

By substituting $\dot{e}(t)$ from (20) and ${}^C D_t^\alpha S(\mathbf{x},t)$ from (24) into expression A, we have

$$A = S(\mathbf{x},t)\left[-k_2(t)\text{sat}S(\mathbf{x},t) + \frac{e(t)}{m_s(t)}\right] + \frac{e(t)}{\overline{m}_s}[\dot{d}(t) - \mathbf{l}(\mathbf{x})\mathbf{g}_2 e(t)]. \tag{29}$$

From (3), (17), and (29), the followings are yielded.

$$\begin{aligned} A &= S(\mathbf{x},t)\left[-k_2(t)\text{sat}S(\mathbf{x},t)+\frac{e(t)}{m_s(t)}\right] \\ &\quad+\frac{e(t)}{\overline{m}_s}\left[\dot{d}(t)-l_2(t)\frac{e(t)}{m_s(t)}\right] \qquad (30) \\ &= -k_2(t)|S(\mathbf{x},t)|+\frac{S(\mathbf{x},t)e(t)}{m_s(t)}+\frac{e(t)\dot{d}(t)}{\overline{m}_s} \\ &\quad-\frac{l_2(t)e^2(t)}{m_s(t)\overline{m}_s} \\ &\leq -k_2(t)|S(\mathbf{x},t)|+\frac{S^2(\mathbf{x},t)+e^2(t)}{2m_s(t)} \\ &\quad+\frac{e^2(t)+\dot{d}^2(t)}{2m_s(t)}-\frac{l_2(t)e^2(t)}{m_s(t)\overline{m}_s}. \qquad (31) \end{aligned}$$

In case of $l_2(t)=k_l\overline{m}_s$, $k_l>1$, due to $|\dot{d}(t)|<\Omega$, the followings can be inferred from (31).

$$A\leq -k_2(t)|S(\mathbf{x},t)|+\frac{S^2(\mathbf{x},t)+2e^2(t)(1-k_l)+\dot{d}^2(t)}{2m_s(t)}, \qquad (32)$$

$$A< -k_2(t)|S(\mathbf{x},t)|+\frac{S^2(\mathbf{x},t)+\Omega^2}{2m_s(t)}. \qquad (33)$$

Finally, from (31) and (33) we can conclude that if $k_2(t)$ and $l_2(t)$ satisfy (34) as below then $\dot{V}_2<0$.

$$\begin{cases} k_2(t)>\dfrac{S^2(\mathbf{x},t)+\Omega^2}{2m_s(t)|S(\mathbf{x},t)|}, \\ l_2(t)=k_l\overline{m}_s,\ k_l>1. \end{cases} \qquad (34)$$

To prevent (34) from getting the irregular case when $|S(\mathbf{x},t)|=0$, $0<\xi\ll 1$ is added into the expression to obtain the form of (21). Thus, $\dot{V}_2<0$, meaning $e(t)\to 0$ (20) and $S(\mathbf{x},t)\to 0$ are Lyapunov asymptotically stable processes such that $|\dot{d}(t)|<\Omega$.

Remark 3: Condition (34) takes the role of a trade-off between the update-laws of the FDSMC via $k_2(t)$ and the DO via $l_2(t)$ to ensure $\dot{V}_2<0$. In this process, fuzzy law (22) also set up a mechanism of adjustment of $k_2(t)$ to enhance the stability of $(x_1(t),x_2(t))\to 0$.

3.4. Control strategy

From Theorems 1 and 2, the control strategy is summarized.

- Set up the suspension via ($\overline{m}_s$, $\underline{m}_s$, k_s, c_s, k_{tn}, c_{tn});
- Optimize the parameters (α, k_1, $\bar{k}_2$, k_l).

imDO-FDSMC

Step 1: Determine state vector $\mathbf{x}(t)$.

Step 2: Update $S(\mathbf{x},t)$ via (7), ${}^{C}D_t^{\alpha}S(\mathbf{x},t)$ via (9), $l_2(t)$ via (21), $k_2(t)$ via (22), $u_c(t)=\hat{d}(t)$ via (16) and $u_s(t)$ via (8).

Step 3: Control $(x_1(t),x_2(t))\to 0$ by determining the current intensity to support the MRD in Fig. 1(b) such that it generates control force $u(t)$ (6).

Return to Step 1

Remark 4: To exploit well the imDO-FDSMC, optimizing (α, k_1, $\bar{k}_2$, k_l) needs to be performed. By selecting a track profile for testing (the one in Figs. 3 and 4 is used in this paper), it is carried out based on the DE method [26] to minimize the objective function (35).

$$J_{DE}(\alpha,k_1,k_2,\bar{k}_2,k_l) = \min\left[\max_{j=1,\ldots,N}|\dot{x}_{2,i}|+\frac{1}{N}\sum_{i=1}^{N}|\dot{x}_{2,i}|\right], \qquad (35)$$

in their variable regions $\alpha\in[0.9,1)$, $k_1>0$, $\bar{k}_2>1$, $k_l>1$, where N is the number of sampling points of $\dot{x}_2$.

4. VERIFYING THE METHOD

First, we determine optimal values of (α, k_1, $\bar{k}_2$, k_l) via MATLAB simulation. Then, the ability of the imDO-FDSMC is analyzed/compared with the corresponding results from the passive suspension and the suspensions controlled by controllers [4,24,27–29]. They are the fuzzy-based predicting sliding controller (FPSC) [4], the adaptive type-2 fuzzy sliding controller (AT2FC) [24], the adaptive prescribed performance controller (APPC), and the skyhook [29]. The parameters in Table 1 are used for simulations. The maximum acceleration A_a, maximum control force A_u, the absolute mean of acceleration M_a and of control force M_u as in (36) are adopted to verify.

$$\begin{cases} A_a=\max\limits_{i=1\ldots N}|\dot{x}_2^i|;\ A_u=\max\limits_{i=1\ldots N}|u^i|, \\ M_a=N^{-1}\sum\limits_{i=1}^{N}|\dot{x}_2^i|;\ M_u=N^{-1}\sum\limits_{i=1}^{N}|\dot{x}_2^i|. \end{cases} \qquad (36)$$

In the above, N is the number of sampling points.

Table 1. The quarter car model parameters.

Parameters	Value	Unit
Nominal chassis mass (m_{sn})	350	kg
Maximum chassis mass ($\overline{m}_s$)	390	kg
Minimum chassis mass ($\underline{m}_s$)	310	kg
Unsprung mass (m_u)	59	kg
Spring stiffness (k_s)	13500	N/m
Damping coefficient (c_s)	1250	Ns/m
Nominal equivalent stiffness (k_{tn})	190000	N/m
Equivalent stiffness (k_t)	$k_{tn}\pm 20\%$	N/m
Nominal equivalent damping (c_{tn})	14500	Ns/m
Equivalent damping coef. (c_t)	$c_{tn}\pm 20\%$	Ns/m

4.1. Parameter optimization

The parameters in Table 1, the track profile (37) and Fig. 3, and unwanted impact of UAD consisting of $d(t)$ and $m_s(t)$ as in (37) and Fig. 4 are all adopted to optimize α, k_1, $\bar{k}_2$, k_l based on the method in Remark 4.

$$\begin{aligned} z_r &= 0.1\sin(\omega t) + 0.004\sin(20\pi t) \\ &\quad + 0.002[\sin(2\pi t) + \sin(7.5\pi t)], \\ d(t) &= 300[\sin(1.5\pi t)\sin(0.15\pi t) \\ &\quad + \cos(0.6\pi t)\sin(0.3\pi t)], \\ m_s(t) &= m_{sn} + 0.05m_{sn}[\sin(0.5\pi t)\sin(0.15\pi t) \\ &\quad + \cos(0.6\pi t)\sin(0.3\pi t)]. \end{aligned} \tag{37}$$

The obtained optimal parameters are $k_1 = 1.34$, $k_l = 1.21$, $\bar{k}_2 = 235.1$ and $\alpha = 0.95$. They will be used for all the surveys in the rest of this paper. The optimization has a vital role in control effectiveness. As an example, Table 2 expresses clearly that the ability of the imDO-FDSMC depends deeply on α; therefore, its optimum value needs to be determined for each specific application.

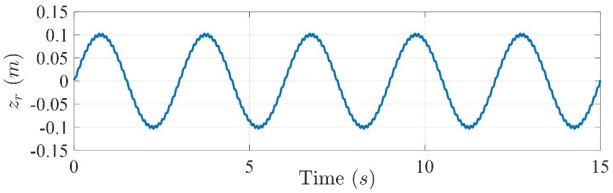

Fig. 3. Sinusoidal track profile.

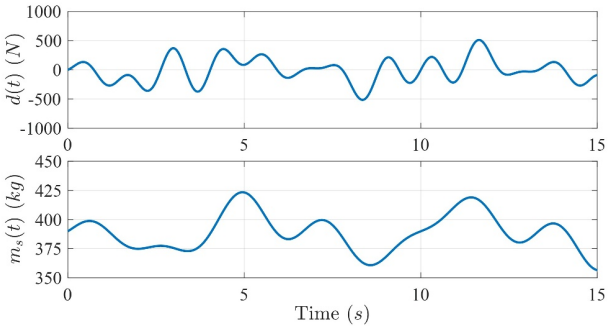

Fig. 4. The external disturbance and randomly varied chassis mass.

Table 2. The role of α.

α	A_a (m/s^2)	M_a (m/s^2)
1.0	0.1694	0.0931
0.99	0.1721	0.0774
0.93	0.1006	0.0519
$\alpha_{op} = 0.95$	0.0742	0.0356

4.2. Simulations

4.2.1 Sinusoidal track profile

The track profile (37) is again used. For the imDO-FDSMC, the two cases with and without the AFL (22) are adopted. The results in Fig. 5 and Table 3 reflect that under the impact of the AFL, $S(t)\dot{S}(t)$ becomes much lower; as a result, chassis acceleration in the case of using the AFL is much smaller than that but without using. So, the AFL will be employed in the rest of this paper. The results in Table 3 are also shown the control ability of the proposed method to be better than the others.

4.2.2 Track profile with two opposite bumps and UAD

An excitation as in Fig. 6 and (38) is employed, where $d_1(t) = 0.002[\sin(2\pi t) + \sin(7.5\pi t)]$ is disturbance.

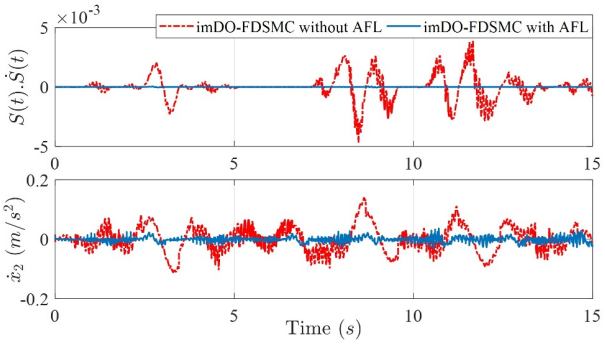

Fig. 5. $S(t)\cdot\dot{S}(t)$ and acceleration of the chassis controlled by the imDO-FDSMC with/without the AFL.

Table 3. Sinusoidal profile: Chassis' vertical acceleration.

Methods	A_a (m/s^2)	M_a (m/s^2)
Passive	1.544839	0.489623
Skyhook	1.340440	0.455658
SARC	0.727523	0.188782
APPC	0.559276	0.206107
AT2FC	0.429106	0.149222
FPSC	0.414792	0.106733
Proposed (with the AFL)	0.361782	0.058835

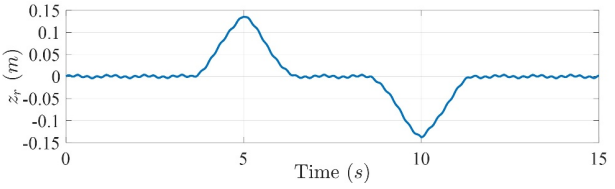

Fig. 6. Track profile with two opposite bumps and UAD.

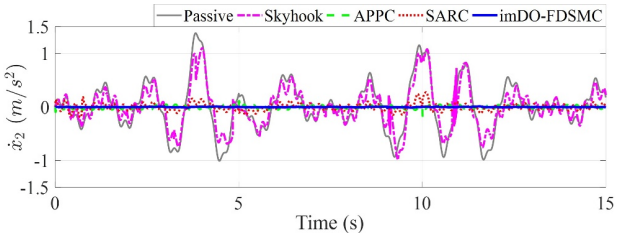

Fig. 7. The vertical acceleration of the chassis.

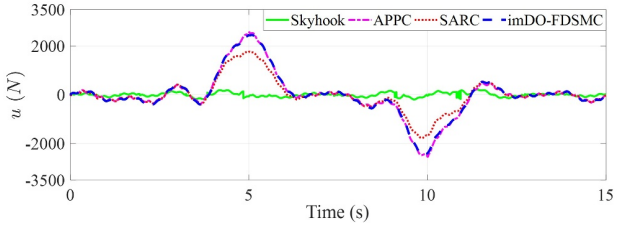

Fig. 8. The control forces.

Table 4. Vertical chassis accelerations and control force.

Methods	A_a (m/s^2)	Max $\lvert u\rvert$ (N)	M_a (m/s^2)	Mean $\lvert u\rvert$ (N)
Passive	1.381371	0	0.365787	0
Skyhook	1.099272	216.33	0.283219	65.89
SARC	0.275502	1778.22	0.052213	419.87
APPC	0.168557	2569.90	0.025509	542.18
Proposed	0.049113	2464.57	0.0052443	545.94

$$z_r(t) = \begin{cases} -0.0592t_1^3 + 0.1332t_1^2 + d_1(t), & \text{if } 3.5 \le t < 5, \\ 0.0592t_2^3 + 0.1332t_2^2 + d_1(t), & \text{if } 5 \le t < 6.5, \\ 0.0592t_3^3 - 0.1332t_3^2 + d_1(t), & \text{if } 8.5 \le t < 10, \\ -0.0592t_4^3 - 0.1332t_4^2 + d_1(t), & \text{if } 10 \le t < 11.5, \\ d(t), & \text{otherwise.} \end{cases} \tag{38}$$

The results from this are shown in Figs. 7-8 and Table 4. Namely, vertical acceleration of the chassis controlled by the imDO-FDSMC is the smallest. Although the peak of the vertical acceleration approaches to the zero vicinity, the control force supported by the proposed stays in a large border quite similar to the force of the APPC but higher than that from the Skyhook.

4.2.3 Track profile constituted of consecutive bumps

A track profile like the speed humps with six consecutive bumps as in Fig. 9 and described mathematically via the velocity of a train-car passing through them as below

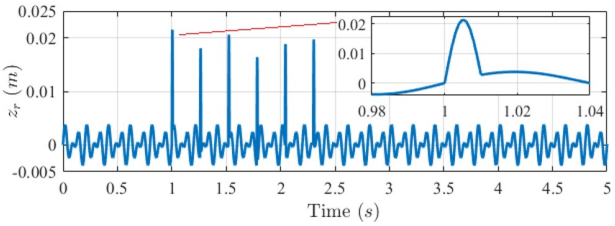

Fig. 9. The track profile like the speed humps.

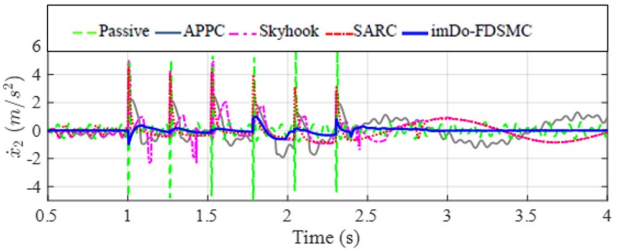

Fig. 10. The chassis' vertical acceleration.

is used to evaluate the controller.

$$z_r(t) = \begin{cases} 0.02\sin[\omega(t-1)] + d_2(t), \\ \quad \text{if } 1 \le t \le 1 + T_D, \\ 0.02\sin[\omega(t-1-T_D-T_W)] + d_2(t), \\ \quad \text{if } 1 + T_D + T_W \le t \le 1 + 2T_D + T_W, \\ 0.02\sin[\omega(t-1-2T_D-2T_W)] + d_2(t), \\ \quad \text{if } 1 + 2T_D + 2T_W \le t \le 1 + 3T_D + 2T_W, \\ 0.02\sin[\omega(t-1-3T_D-3T_W)] + d_2(t), \\ \quad \text{if } 1 + 3T_D + 3T_W \le t \le 1 + 4T_D + 3T_W, \\ 0.02\sin[\omega(t-1-4T_D-4T_W)] + d_2(t), \\ \quad \text{if } 1 + 4T_D + 4T_W \le t \le 1 + 5T_D + 4T_W, \\ 0.02\sin[\omega(t-1-5T_D-5T_W)] + d_2(t), \\ \quad \text{if } 1 + 5T_D + 5T_W \le t \le 1 + 6T_D + 5T_W, \\ d_2(t), \quad \text{otherwise.} \end{cases}$$

In the above, $T_D = \frac{D}{v}$ s, $T_W = \frac{W}{v}$ s; $D = 0.1$ m is the bump width; $W = 2.5$ m is the step distance between the two consecutive bumps; $v = 10$ m/s is the train-car velocity; $d_2(t) = 0.002[\sin(30\pi t) + \sin(20\pi t)]$ denotes the rough surface.

The results in Figs. 10-11 and Table 5 illustrate that controlled by the imDO-FDSMC the train-car could cross through the intense terrain with the chassis acceleration to be maintained in low amplitude and stamped out quickly.

4.3. Evaluating the method via an experimental apparatus

The experimental apparatus as in Fig. 12 is employed. The hydraulic exciter makes displacement at the wheel. It then makes the upper-bed vibrate vertically via the sus-

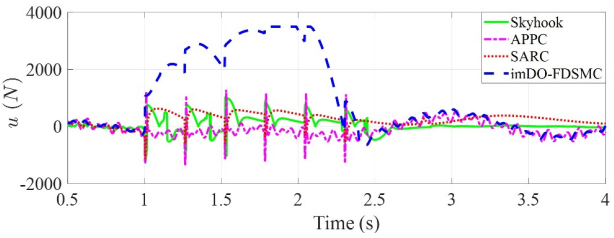

Fig. 11. The control forces.

Table 5. Chassis acceleration and control force.

Methods	A_a (m/s^2)	M_a (m/s^2)	Max $\|u\|$ (N)	Mean $\|u\|$ (N)
APPC	4.483555	0.442549	4.483555	0.442549
Skyhook	4.985060	0.385575	4.985060	0.385575
SARC	4.547051	0.374275	4.547051	0.374275
Passive	5.996610	0290423	5.996610	0.290423
Proposed	0.974527	0.052058	0.974527	0.052058

pension. The suspension here is constituted of an MRD and a spring. Displacement $x_1(t)$ of the upper-bed and the relative displacement (d_{re}) between the upper-bed and the wheel are measured by an LVDT (linear variable differential transformer) sensor. Acceleration of the upper-bed $\dot{x}_2(t)$ is determined by the coordination of an IEPE (Integrated Electronics Piezo-Electric) sensor, NI 9234, and the computer which work as an accelerometer. The computer is also used to make the hydraulic excitation, establish control laws, and set up an inverse-MRD model as mentioned in [1].

Be noted that the structure and operating principle of the system in Fig. 12 is similar to that of the MRD-based suspension in Fig. 1(b). The mass $m_s = 246.5 \pm 35$ kg is set up at the upper bed; made vibration with an amplitude of 0.025 m and a frequency of 2Hz at the wheel. Surveys are then performed to obtain Table 6. The results from the table again reflect the positive role of the imDO-FDSMC. Among the surveyed methods, the capability of the pro-

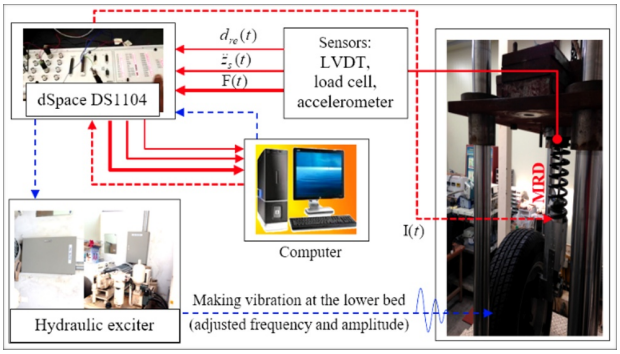

Fig. 12. The block diagram of the control system for the semi-active MRD suspension, a quarter-car model.

Table 6. Vertical acceleration of the upper bed.

Methods	A_a (m/s^2)	M_a (m/s^2)
Passive	0.2594	0.0978
AT2FC	0.1237	0.0641
APPC	0.1180	0.0508
FPSC	0.0974	0.0489
Proposed	0.0842	0.0456

posed method to stamp out the vibration is the best.

Collaborating with Subsection 4.2, it can easily be observed that although the effectiveness of the proposed method is the best, unlike the simulations, in the real application, the compared effectiveness of the imDO-FDSMC is not too much. It relates to the time-delay due to the larger calculation cost.

5. CONCLUSION

The compensator-enhanced FD sliding control of a class of SD-TCSs subjected to UAD whose disturbance time-varying rate may be high but bounded has been presented. It was constituted of the FD-based sliding mode controller FDSMC for controlling the SD-TCSs without UAD and the imDO for compensating for UAD. Some aspects observed from the surveys are as follows:

• Compared with the considered methods, i) the control performance of the imDO-FDSMC reflected via the ability to stamp out the chassis vibration stably is the best; ii) the control force used by the proposed method is however not smallest which is quite similar to the force utilized by the APPC.

• The imDO-FDSMC is able to adjust itself adaptively to improve control effectiveness. The optimal values of its main parameters (α, k_1, $\bar{k}_2$, k_l) can be determined easily by simulation.

• Because the FD equation is a generalization of the differential equation, the design of control systems based on FD can be seen as a general approach, from which one may obtain FD-based systems or integer-order derivative-based systems depending on the optimal result $\alpha = \alpha_{op}$.

• Be noted that even if alpha is very close to 1, the differentiable attribute cannot be guaranteed. Without loss of generality, when the solution of (2) is not an integer-order derivative, the extended Caputo derivative of [10,11] should be considered. Besides, the time delay due to the calculation cost of the proposed method is an issue needing to be improved. The approach based on the extended Caputo derivative considering the impact of the time delay will be presented in our next research.

REFERENCES

[1] S. D. Nguyen, W. H. Kim, J. H. Park, and S. B. Choi,

"A new fuzzy sliding mode controller for vibration control systems using integrated-structure smart dampers," *Smart Materials and Structures*, vol. 26, pp. 1-16, 2017.

[2] S. D. Nguyen, S. B. Choi, and T. I. Seo, "Adaptive fuzzy sliding control enhanced by compensation for explicitly unidentified aspects," *International Journal of Control, Automation, and Systems*, vol. 15, pp. 2906-2920, 2017.

[3] Y. Qin, F. Zhao, Z. Wang, L. Gu, and M. Dong, "Comprehensive analysis for influence of controllable damper time delay on semi-active suspension control strategies," *Journal of Vibration and Acoustics*, vol. 139, no. 3, p. 031006, 2017.

[4] S. D. Nguyen and T. I. Seo, "Establishing ANFIS and the use for predicting sliding control of active railway suspension systems subjected to uncertainties and disturbances," *International Journal of Machine Learning and Cybernetics*, vol. 9, no. 5, pp. 853-865, 2016.

[5] W. H. Chen, "Nonlinear disturbance observer-enhanced dynamic inversion control of missiles," *Journal of Guidance, Control, and Dynamics*, vol. 26, no. 1, pp. 161-166, 2003.

[6] S. D. Nguyen, B. D. Lam, and S. B. Choi, "Smart dampers-based vibration control - Part 2: Fractional-order sliding control for vehicle suspension system," *Mechanical Systems and Signal Processing*, vol. 148, p. 107145, 2020.

[7] A. C. Norelys, A. D. M. Manuel, and A. G. Javier, "Lyapunov functions for fractional order systems," *Communications in Nonlinear Science and Numerical Simulation*, vol. 19, no. 9, pp. 2951-2957, 2014.

[8] S. D. Nguyen, B. D. Lam, and V. H. Ngo, "Fractional-order sliding-mode controller for semi-active vehicle MRD suspensions," *Nonlinear Dynamics*, vol. 101, pp. 795-821, 2020.

[9] C. Li and W. Deng, "Remarks on fractional derivatives," *Applied Mathematics and Computation*, vol. 187, pp. 777-784, 2007.

[10] A.-J. Muñoz-Vázquez, V. Parra-Vega, A. Sánchez-Orta, and G. Romero-Galván, "Quadratic Lyapunov functions for stability analysis in fractional-order systems with not necessarily differentiable solutions," *Systems & Control Letters*, vol. 116, pp. 15-19, 2018.

[11] A.-J. Muñoz-Vázquez, V. Parra-Vega, and A. Sánchez-Orta, "Non-smooth convex Lyapunov functions for stability analysis of fractional-order systems," *Transactions of the Institute of Measurement and Control*, vol. 41, no. 6, pp. 1627-1639, 2019.

[12] H. You, Y. Shen, H. Xing, and S. Yang, "Optimal control and parameters design for the fractional-order vehicle suspension system," *Journal of Low Frequency Noise, Vibration and Active Control*, vol. 37, no. 3, pp. 456-467, 2018.

[13] P. Wang, Q. Wang, X. Xu, and N. Chen, "Fractional critical damping theory and its application in active suspension control," *Shock and Vibration*, vol. 2017, Article ID 2738976, 2017.

[14] Z. Zhu, Y. Pan, Q. Zhou, and C. Lu, "Event-triggered adaptive fuzzy control for stochastic nonlinear systems with unmeasured states and unknown backlash-like hysteresis," *IEEE Transactions on Fuzzy Systems*, vol. 29, no. 5, pp. 1273-1283, 2021.

[15] W. Wang, H. Liang, Y. Pan, and T. Li, "Prescribed performance adaptive fuzzy containment control for nonlinear multiagent systems using disturbance observer," *IEEE Transactions on Cybernetics*, vol. 50, no. 9, pp. 3879-3891, 2020.

[16] S. D. Nguyen, S. B. Choi, and T. I. Seo, "Recurrent mechanism and impulse noise filter for establishing ANFIS," *IEEE Transactions on Fuzzy Systems*, vol. 26, no. 2, pp. 985-997, 2017.

[17] S. P. Utkarsh, D. C. Sushant, P. D. Shendge, and S. B. Phadke, "Linear disturbance observer based sliding mode control for active suspension systems with non-ideal actuator," *Journal of Sound and Vibration*, vol. 442, no. 3, pp. 428-444, 2018.

[18] F. J. Lin, K. K. Shyu, and R. J. Wai, "Recurrent fuzzy neural network sliding mode controlled motor toggle servomechanism," *IEEE/ASME Transactions on Mechatronics*, vol. 6, no. 4, pp. 453-466, 2001.

[19] S. Roy, S. B. Roy, J. Lee, and S. Baldi, "Overcoming the under- and over-estimation problems in adaptive sliding mode control," *IEEE/ASME Transactions on Mechatronics*, vol. 24, no. 5, pp. 2031-2039, 2019.

[20] S. Kurode, S. K. Spurgeon, B. Bandyopadhyah, and P. S. Gandhi, "Sliding mode control for slosh-free motion using a nonlinear sliding surface," *IEEE/ASME Transactions on Mechatronics*, vol. 18, no. 2, pp. 714-724, 2013.

[21] Y. F. Li, B. Eriksson, and J. Wikander, "Sliding mode control of two-mass positioning systems," *Proc. of the 14th IFAC Triennial World Congress*, Oxford, pp. 151-156, 1999.

[22] J. J. Kim, J. J. Lee, K. B. Park, and M. J. Youn, "Design of a new time-varying sliding surface for robot manipulator using variable structure controller," *Electronics Letters*, vol. 29, no. 2, pp. 195-196, 1993.

[23] S. Tokat, M. S. Fadali, and O. Eray, "A classification and overview of sliding mode controller sliding surface design methods," *Studies in Sysems, Decision and Control*, vol. 24, pp. 417-439, 2015.

[24] S. D. Nguyen, D. Jung, and S. B. Choi, "A robust vibration control of a magnetorheological damper based railway suspension using a novel adaptive type-2 fuzzy sliding mode controller," *Shock and Vibration*, vol. 2017, Article ID 7306109, 2017.

[25] X. Lei, *High Speed Railway Track Dynamics: Models, Algorithms and Applications*, Science Press, Beijing, Springer Nature Singapore Pte Ltd., pp. 271-280, 2017.

[26] W. Gong and Z. Cai, "Differential evolution with ranking-based mutation operators," *IEEE Transactions on Cybernetics*, vol. 43, no. 6, pp. 2066-2081, 2013.

[27] W. Sun, Z. Zhao, and H. Gao, "Saturated adaptive robust control for active suspension systems," *IEEE Transactions on Industrial Electronics*, vol. 60, no. 9, pp. 3889-3896, 2013.

[28] C. Hua, J. Chen, Y. Li, and L. Li, "Adaptive prescribed performance control of half-car active suspension system with unknown dead-zone input," *Mechanical Systems and Signal Processing*, vol. 111, pp. 135-148, 2018.

[29] H. Zhang, E. Wang, F. Min, R. Subash, and C. Su, "Skyhook-based semi-active control of full-vehicle suspension with magneto-rheological dampers," *Chinese Journal of Mechanical Engineering*, vol. 26, no. 3, pp. 498-505, 2013.

Sy Dzung Nguyen received his M.E. degree in manufacturing engineering from Ho Chi Minh City University of Technology (HCMUT) – VNU in 2001, a Ph.D. degree in applied mechanics in 2011 from HCMUT. He was a postdoctoral fellow at Inha University, Korea, 2011-2012, at Incheon National University, Korea, 2015-2016. He is currently a Head of Division of Computational Mechatronics (DCME), Institute for Computational Science (INCOS), Ton Duc Thang University (TDTU), Vietnam. His research interests include artificial intelligence and its applications to nonlinear adaptive control, system identification, and managing structure damage. Dr. Nguyen has been the main author of plenty of ISI papers in these fields.

Vien Quoc Nguyen received his B.E. and M.E. degrees in automatic control engineering from Ho Chi Minh City University of Technology (HCMUT), Vietnam, in 1998 and 2003. He received a Ph.D. degree in mechanical engineering in 2010 from Inha University, Korea. He is currently with the Mechatronic Division, Faculty of Mechanical Engineering at Industrial University of Ho Chi Minh City, Vietnam. His research interests include nonlinear adaptive control, vibration control, smart materials, and their applications.